LESE
LABORATORY FOR EARTHQUAKE AND STRUCTURAL ENGINEERING

Out-of-plane seismic response of stone masonry walls: Analytical study of real piers

Tiago Ferreira

Department of Civil Engineering – University of Aveiro

Alexandre Costa

Department of Civil Engineering – Faculty of Engineering - University of Porto

LESE 02/2012
October 2012

Out-of-plane seismic response of stone masonry walls: Analytical study of real piers

TIAGO MIGUEL FERREIRA

UNIVERSITY OF AVEIRO

ALEXANDRE COSTA

FACULTY OF ENGINEERING OF THE UNIVERSITY OF PORTO

LESE REPORT 02/2012

Faculty of Engineering of the University of Porto

OCTOBER 2012

ABSTRACT

This report presents the application of a simplified displacement-based procedure to the characterization of the nonlinear force-displacement relationship for the out-of-plane behavior of unreinforced traditional masonry walls. According to this procedure, tri-linear models based on three different energy based criteria were constructed and confronted with three experimental tests on existing stone masonry constructions.

Moreover, a brief introduction is presented regarding the main characteristics of the *in situ* cyclic testing recently carried out using distributed loads, as well as results obtained during the experimental campaigns performed. The comparison between the experimental and the analytical results are presented and discussed.

Finally a new experimental campaign test, currently under preparation, is briefly described in terms of expected results and new developments for the analytical procedure presented in the report.

CONTENTS

1 INTRODUCTION

Recent earthquakes around the world, including the Azores archipelago (Portugal), have identified the out-of-plane collapse of URM walls as one of the most important failure modes. This suggests that existing URM walls may be vulnerable to future earthquakes and should be studied for their seismic resistance. Thus, during the last years, several studies focused on the seismic response of masonry structures as well as on its structural retrofitting. A wide range of approaches from analytical modelling to extensive experimental and numerical methods have been used, where micro-models as well as single and multi-degree-freedom (MDOF) macro-models have been applied in this kind of analysis ((Kelly, 1995); (Lam, Wilson, & Hutchinson, 1995); and (Blaikie & Davey, 2002)).

For simplicity, the behaviour of a wall subjected to out-of-plane forces may be modelled as a SDOF system ((Doherty, Griffith, Lam, & Wilson, 2002); and (Derakhshan, Ingham, & Griffith, 2009)). In fact, several researchers have studied the out-of-plane behaviour URM walls using this formulation and actually, all the nonlinearities associated with the material and construction practice of the URM walls, and the uncertainties involved in the selection of appropriate parameters for a complex numerical analysis, may render micro-modelling ineffective (Derakhshan et al., 2009). In this report, a SDOF idealization of the rocking behaviour of URM walls based on their force-displacement (F-Δ) relationship is presented and described. This idealization was developed and is applied to URM cantilever walls.

2 PRESENTATION OF A SIMPLIFIED DISPLACEMENT-BASED PROCEDURE

2.1 Introduction

The simplified displacement-based procedure developed and applied in this work is based on the tri-linear F-Δ relationship originally described by Lam, Griffith, Wilson and Doherty (2003). This original formulation was based on statics assuming rigid body behaviour of the wall and neglecting the effects of its deformation and degradation. Based on this F-Δ relationship, a tri-linear model can be constructed for a one-way out-of-plane URM wall, knowing its mass, boundary conditions, overburden and dimensions.

To construct the tri-linear model, two ratios $\Delta_1/\ \Delta_f$ and $\Delta_2/\ \Delta_f$ are used in conjunction with the bi-linear rigid body model of the wall. The displacement values Δ_1 and Δ_2 control respectively the initial stiffness reduction and strength reduction and Δ_f represents the maximum stable displacement (see Fig. 1).

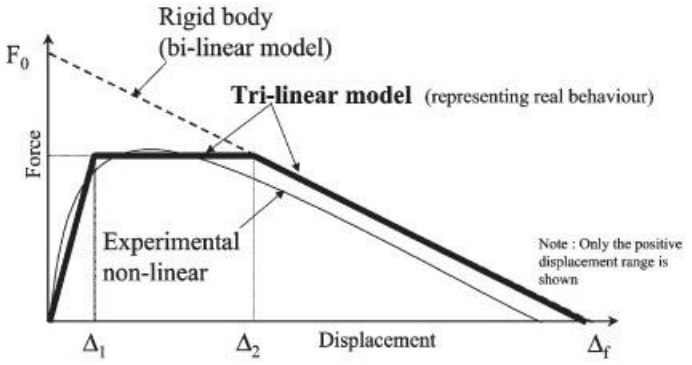

Tri-linear model parameters

Condition	$\frac{\Delta_1}{\Delta_f}$	$\frac{\Delta_2}{\Delta_f}$
New	6%	28%
Moderate	13%	40%
Severe	20%	50%

Fig. 1: Bi-linear and tri-linear force displacement models (adapted from Lam et al. (2003))

In summary, Δ_1, Δ_2, Δ_f and F_0 are the only input parameters needed to define the tri-linear F-Δ relationship forming the macro SDOF model. Values for F-Δ and F_0 (according to Eqn. (1)) are first determined to construct the bi-linear spine based on the wall dimensions, boundary conditions and overburden loading conditions. The final tri-linear relationship is then defined according to representative values of Δ_1 and Δ_2 which account for the real non-linear behaviour of the wall (Lam et al., 2003).

2.2 Construction of the bi-linear rigid body model

In this section the static response of a freestanding unreinforced masonry wall – cantilever wall - is described and its representation as an equivalent single degree-of-freedom system developed. Considering rigid-body behaviour of a freestanding wall, it is possible to describe its behaviour using basic principles of static equilibrium.

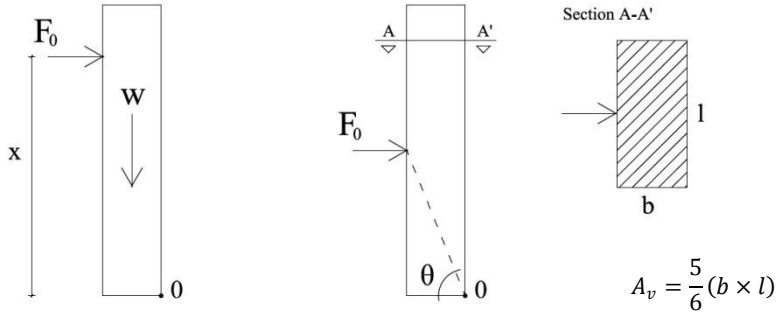

Fig. 2: Forces and reactions on rigid URM parapet walls

Based on Fig. 2 and considering the overturning equilibrium of the wall about the pivot point *O* located at the base of the wall, it is possible to obtain the force of incipient rocking (F_0) according to Eqn.(1):

$$F_0 = \frac{M \times t}{2x} \tag{1}$$

where *M* is the total mass of the wall, *t*, the wall thickness and *x*, the height of the distributed load resultant. For the cases which the wall slenderness ratio is low and the resultant of the horizontal distributed forces is applied at mid-height of the wall (Fig. 2(b)) – as in the case of airbag testing (see section 3.1, test 1) - the value of the force of incipient rocking should be incremented due to the development of a compression strut located at the base of the wall. The value of this compression force may be calculated using Eqn.(2):

$$R = F_0 \times A_v \times \tan(\theta) \tag{2}$$

where F_0 is force of incipient rocking; A_v, the horizontal cross-section area; and θ, the masonry angle of the internal friction (in accordance to Betti and Vignoli (2008)), the value of variable θ adopted in this work was equal to 38º). Figure 2 shows the forces involved in the formulations analytically described by Eqn. (1) and Eqn.(2). Note that it is expected that the cantilever wall shown in Fig. 2 experiences instability when Δ_f equals or exceeds a certain displacement value dependent on the position of resultant *x*. This displacement value corresponds to the moment when the centre of gravity of wall is vertical above the pivoting point, 0, and the resistance of the wall to overturning is zero. In this work, only the thickness of the outside leaf of the wall was used as maximum stability displacement, Δ_f. The use of this value is properly reasoned in A. A. Costa (2012) based on shaking table tests evidence.

2.3 Calibration of parameters Δ_1 and Δ_2 based on energy criteria

In order calibrate the displacement limit values Δ_1 and Δ_2 based on experimental tests, three energy based criteria were defined. The first criterion, named as "Experimental Fit Curve", considers the energy balance to the offset value corresponding to the maximum experimental envelope (in strength), d_{Fmax}. Fig. 3 shows schematically the first energy based criterion.

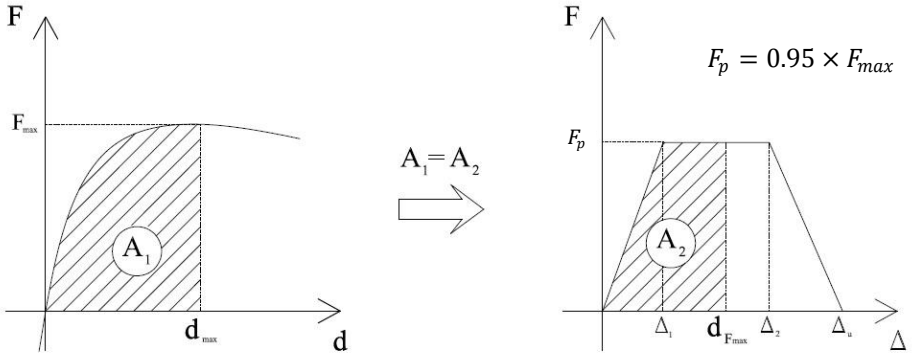

Fig. 3: Energy balance to the offset value d_{Fmax}: (a) Experimental envelope; (b) Tri-linear approximation

Note that in this formulation the maximum strength value considered in the tri-linear model, F_p, is equal to 95% of the maximum strength value attained experimentally, F_{max}. On the following, the step-by-step construction of the tri-linear model, according to the first energy based criterion, is described:

i. Determination of the area A_1;

ii. Construction of the bi-linear model F_0-Δ_u according to the exposed in Sec. 2.1;

iii. Definition of nonlinear plateau considering that the maximum analytical force, F_p, is equal to 95% of the maximum experimental force, F_{max}. The limit displacement value Δ_2 is properly defined through the construction of the bi-linear model F_0-Δ_u in step ii.;

iv. Definition of the offset value d_{Fmax} as the boundary for the energy balance of area A_2;

v. Adjustment of the initial analytic stiffness until the energy balance (A_1=A_2) is achieved.

The second formulation, named as "d_f curve", is based on two assumptions: (i) the initial stiffness value is set at 70% of the maximum experimental strength value (according to NTC2008 (2008)); and (ii) the values of $F_{máx}$ and P – the nonlinear *plateau* - are defined considering the energy balance to the offset value corresponding to 20% loss of strength after the maximum value of the experimental force (F=0.8·F_{max}); following these two steps, it is possible to define, in an approximate way, the limit displacement values Δ_1 and Δ_2. Fig. 4 shows the energy based criterion described above.

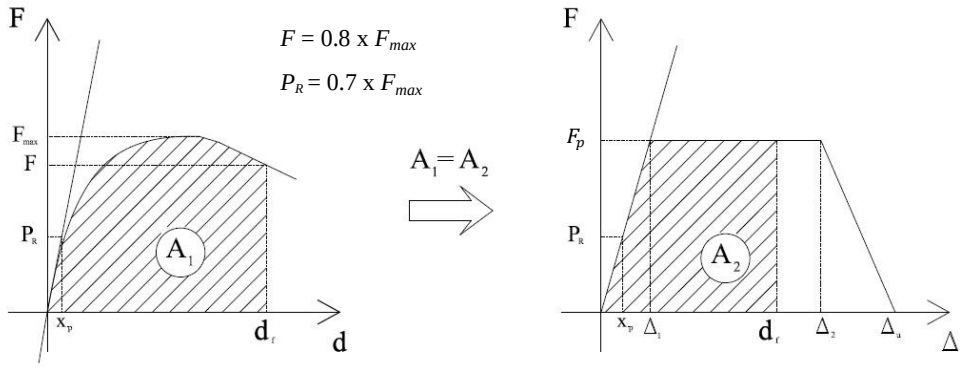

(a) (b)

Fig. 4: Energy balance to the offset value corresponding to 20% loss of strength after F_{max}: (a) Experimental envelope; (b) Tri-linear approximation

According to this second energy based criterion, the tri-linear model can be constructed according to the following procedure:

i. Determination of the area A_1, considering as limit displacement value d_f, the displacement corresponding to a value of force equal to 80% of the maximum experimental strength, F_{max};

ii. Consider in the model an initial stiffness value of 70% of the experimental stiffness value;

iii. Construction of the bi-linear model F_0-Δ_u according to the exposed in Sec. 2.1;

iv. Use the limit displacement value, d_f, as boundary to fix area A_2.

v. Equalize areas A_1 and A_2, vertically adjusting the nonlinear *plateau* (max. analytical force, F_p).

Finally, the third formulation (see Fig. 5), named as "Δ_2 curve", consider the energy balance to the offset value of Δ_2, setting the initial stiffness at 70% of the maximum experimental strength value, F_{max} (NTC2008, 2008). As in the previous formulation, F_p is defined here through energy balance (A_1=A_2).

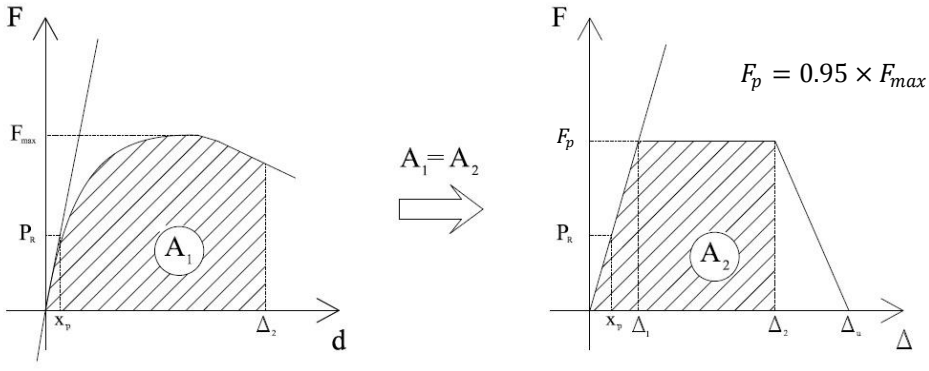

(a) (b)

Fig. 5: Energy balance to the offset value Δ_2, setting the stiffness at 70% of the maximum experimental strength value, F_{max}: (a) Experimental envelope; (b) Tri-linear approximation

The step-by-step construction of the tri-linear model, according to the third energy based criterion, is the following:

i. Start constructing the bi-linear model F_0-Δ_u according to the exposed in Sec. 2.1;

ii. Consider in the model an initial stiffness value of 70% of the experimental stiffness value;

iii. Start the following iterative process:

   a. Define the limit displacement value Δ_2 through the vertical adjustment of the maximum analytical force, F_p;

   b. Determine area A_2 and compare it with area A_1 considering Δ_2 as one of its horizontal boundaries;

   c. If: $A_1 = A_2$ then energy balance was obtained and the process is finished; else If: $A_1 \neq A_2$ restart the iterative process from step a.

3 APPLICATION OF THE SIMPLIFIED DISPLACEMENT-BASED PROCEDURE

3.1 Experimental tests: presentation and description

This section briefly presents the three experimental tests, previously carried out by the author and used in this work on the application of the simplified displacement-based procedure presented in Sec.2. The experimental tests used as case study were carried out on typical masonry houses from Azores, constituted by double leaf basalt stone masonry with poor infill – also known as "*sacco*" masonry (see Fig. 6). Although these buildings normally present 1, 2 or 3 floors at maximum, they are seismically very vulnerable, as proved by the earthquake that hit the archipelago on the 9th July 1998.

Fig. 6: Typical Azorean masonry houses used in the experimental tests

The first experimental test used as case study was performed using a test setup based on previous proposals by other authors (Griffith, Vaculik, Lam, Wilson, & Lumantarna, 2007) which consists of applying one airbag on each side of the wall, in order to mobilize its out-of-plane response under quasi-static cyclic loads. Taking into account the difficulties inherent to *in situ* tests, three fundamental orientation lines were defined: (i) the test setup should be self-equilibrated; (ii) with high level of load capacity; and (iii) able to perform out-of-plane tests. Concerning its versatility and straightforward implementation, the testing system was designed to work with simple and light components (less than 30 kg), avoiding external reaction elements to the existing structure (self-equilibrated system). The support structure which transmit the loads to the reaction wall was composed by tubular steel elements (ϕ=60 mm). Besides the metallic elements, there are two reaction surfaces to the airbags, constituted by wood elements and marine plywood plates. Fig. 7 presents the *in situ* implementation for tests and the operation scheme of the airbags on the wall.

(a)

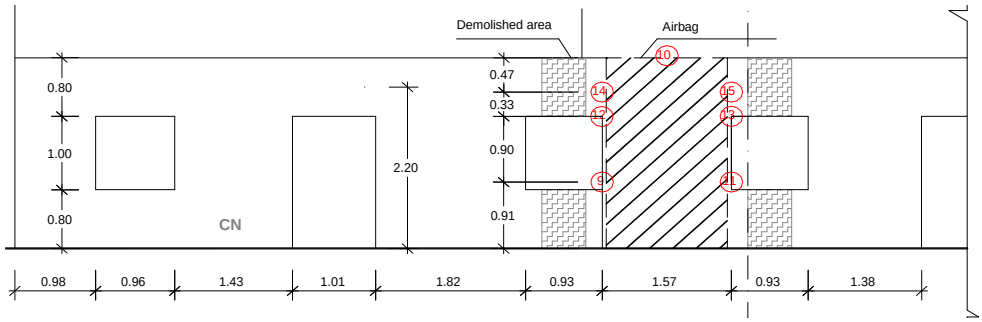

(b)

Fig. 7: Test #1: (a) *in situ* test; and (b) façade and monitored points

The test setup developed makes use of three airbags on each sides of the wall, one compressor, a series of pipes (ϕ=8 mm and ϕ=14 mm) to inflate the airbags, pressure-control valves, displacement and pressure transducers properly connected to data acquisition plates hooked up to a desktop. As already noted, the application of the distributed loads on this kind of test is not new have already been used in the past by other authors. However, the way how the test setup was implemented in experimental campaign, associated with an original structural configuration of the reaction system which allows

bigger displacements, could constitute a step forward in this kind of tests.

The airbag pressure was slowly increased from 0 to the maximum value of about 6.4 kPa for which a maximum horizontal top displacement value of approximately 180 mm was reached. At this displacement point (monitored point 10; Fig. 7(b)), the test ended due to setup limitations in terms of maximum displacement. Fig. 8 shows the hysteretic cycles of force vs. displacement (Fig. 8(a)) as well as representation of the extreme displacement situation of the wall during the test (Fig. 8(b)).

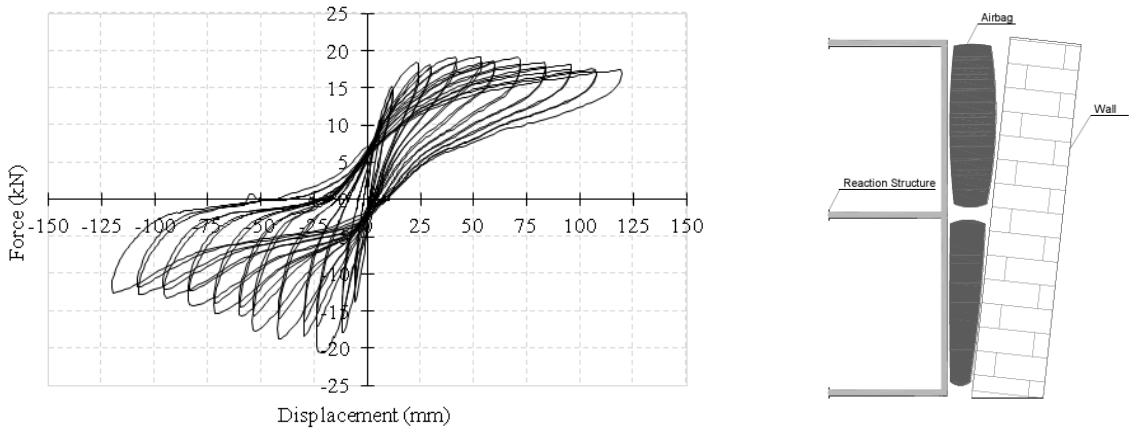

(a) (b)

Fig. 8: (a) Experimental envelope of test 1: distributed loads; and (b) extreme displacement situation in the test

As for the case of the first test, the second and third tests presented here were developed and adopted by the authors specially to assess the out-of-plane behaviour of masonry walls. Again, this is a self-equilibrating setup which presents as great advantage the absence of a specific external reaction structure, using the existing structural elements to provide the required reaction. Fig. 9 presents the test setup used to assess the out-of-plane performance of masonry walls.

(a) (b)

Fig. 9: Experimental test setup used in test #2 and test #3: (a) schematic representation of setup; and (b) *in situ* implementation for tests (interior view) (A. A. Costa, Arêde, Costa, & Oliveira, 2011)

As shown in Fig. 9 and described above, the strongest wall serves as reaction structure, whereas the other wall (main façade in these two cases) is the tested element. Hydraulic devices are placed at the top of the walls and connected to them through hinged links ensuring well-known acting loads and restrain conditions (A. A. Costa et al., 2011). The two tested constructions are similar concerning both in-plane wall distribution, height (one storey) and construction typology and materials. Pictures, schematic layouts and monitoring schemes are included in Fig. 10 and Fig. 11 with reference to the tested elements and to actuators' position.

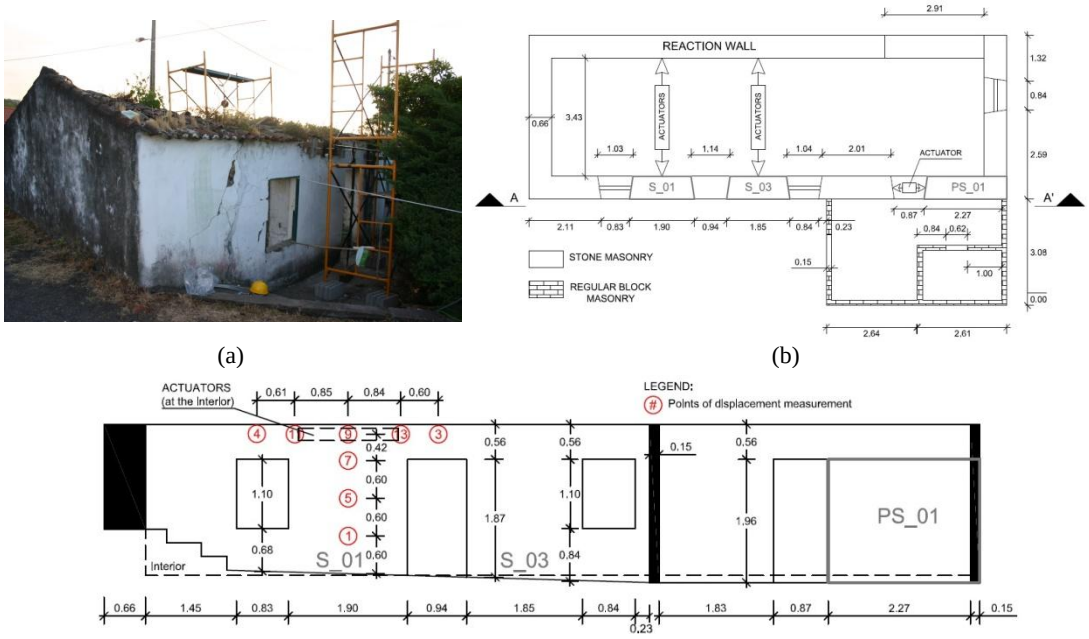

Fig. 10: Test #2: (a) main façade picture; (b) plan view; and (c) main façade (A-A') with displacement monitored points (numbered cycles)

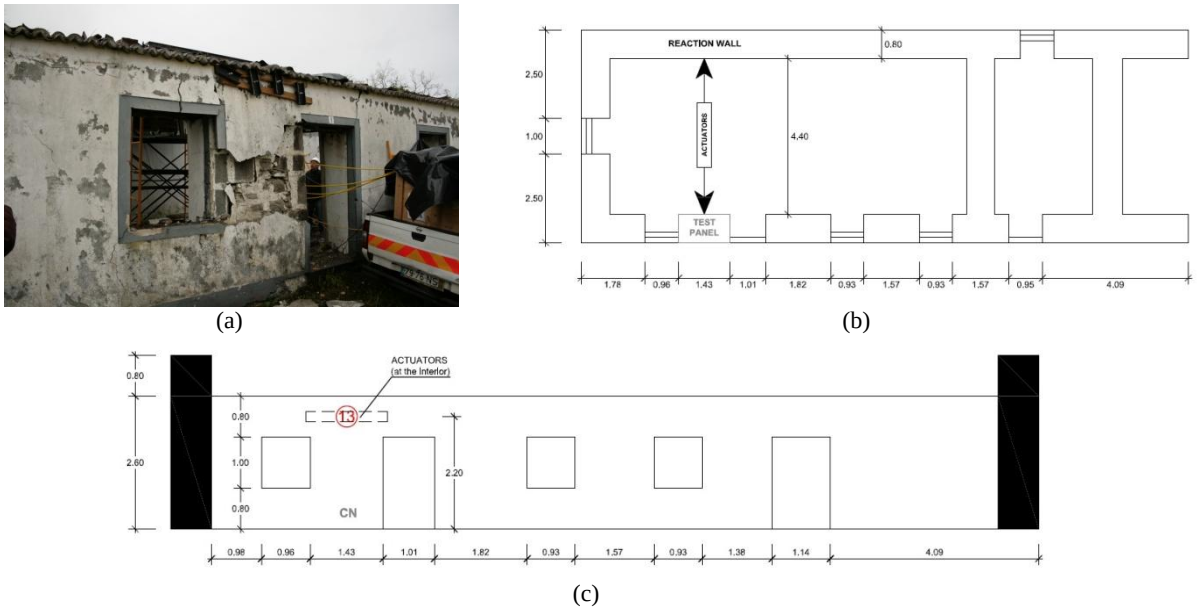

Fig. 11: Test #3: (a) main façade picture; (b) plan view; and (c) main façade

Fig. 12 presents the force vs. displacement curves obtained for the walls (Test #2 and Test #3). Each also includes the maximum expected envelope resulting from rigid-body overturning of the mobilized part of the wall (central pier and two adjacent spandrel beams) (A. A. Costa et al., 2011).

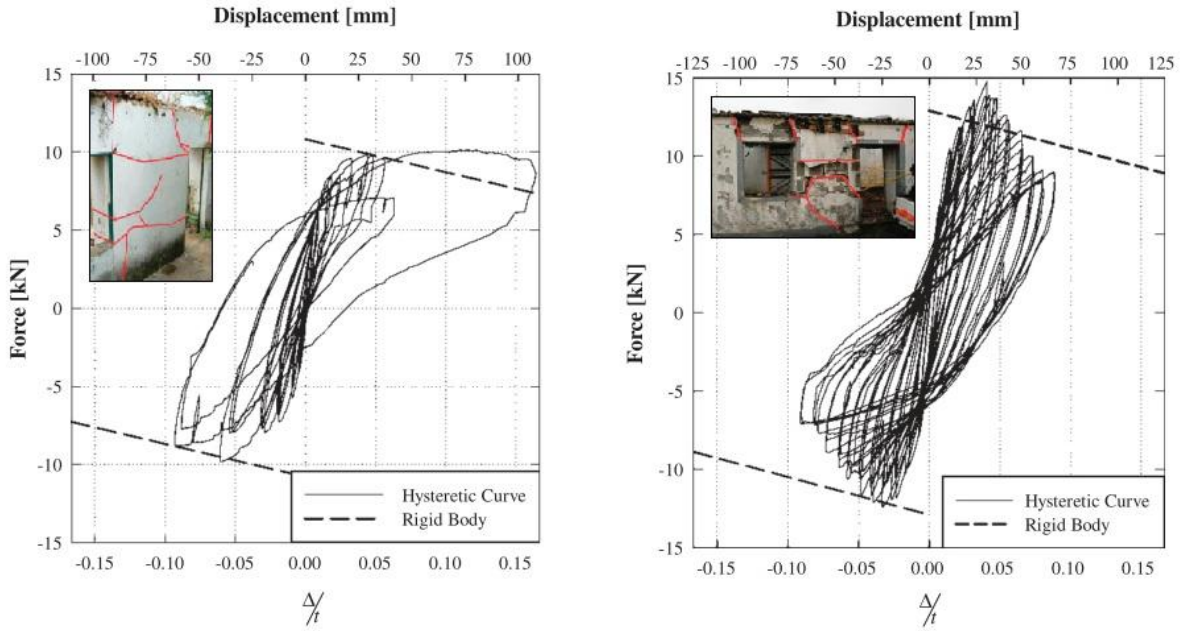

(a) (b)

Fig. 12: Force vs. displacement curves (superimposed with rigid-body motion maximum envelopes), response envelopes and exterior main cracking pattern for the URM walls: (a) Test #2; and (b) Test #3

From the analysis of Fig. 12 it is possible to conclude that the out-of-plane response of the tested walls was characterized by a significant displacement capacity, with horizontal and diagonal cracks both along the wall and the connections to spandrel beams, particularly for Test #2. However, significant strength degradation was observed after the achievement of maximum strength, especially in the case of Test #3, where several cycles highlight this behaviour.

The amount of data obtained from these experimental tests was fundamental in the development and calibration of the new proposals presented in this work. At a first stage it was used in the definition of the kick-off values for the construction of the tri-linear model - Δ_1, Δ_2 and Δ_f – which were subsequently compared with other existing proposals for these parameters (see Table 1). Afterwards, it was used in the calibration of the new energy criteria presented here in Subsect. 2.3.

3.2 Application of the tri-linear model

In this subsection two application of tri-linear model introduced in Sect. 2.1 and 2.2 will be presented. With the first application, a comparative analysis between the limit displacement parameters (Δ_1 and Δ_2) obtained from the direct application of model in the tested URM masonry walls and the parameters

proposed by another authors - for the cases of URM masonry walls with different morphological and physical characteristics - was intended. The second application consisted in the construction of the tri-linear model following the methodologies presented in Sect. 2.3 and its subsequent comparison with the experimental results presented in Sect. 3.1.

Fig. 13 presents the tri-linear models resultant from the first application. This tri-linear model was constructed based on the results obtained from the experimental tests carried out on Test #1 (airbag testing), considering a specific weight of 19 kN/m^3. This value was chosen according to the recommended by (A. Costa, 2002) for this type of material and is consistent with the Italian Code (NTC2008, 2008) for materials with these characteristics. The displacement value Δ_1 was obtained directly from the experimental response envelope and Δ_2 from the intersection point between the bi-linear model spine and the ultimate resistance of an idealised envelope F_u. According to Tomaževič, (1999), this value can be assumed as 90% of the maximum resistance, F_{max}.

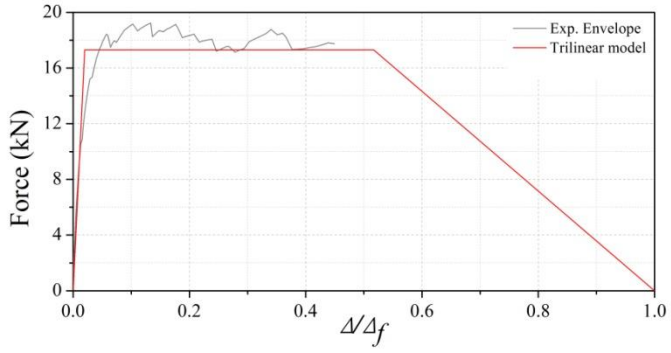

Fig. 13: Comparison between experimental force displacement curves and tri-linear force displacement model

According to this procedure is then possible to obtain new displacement values, Δ_1 and Δ_2, calibrated for "*sacco*" stone masonry. As expected, for the tested URM wall (Test #1), the ratios of $\Delta_1/\ \Delta_f$ and $\Delta_2/\ \Delta_f$ (see Fig. 13) vary significantly from the values suggested by other authors (Derakhshan & Ingham, 2008; Derakhshan et al., 2009; Doherty et al., 2002), especially in the case of $\Delta_2/\ \Delta_f$. This confrontation is shown in Table 1.

Table 1: Different proposes for the tri-linear model parameters

	Parameter	
Reference	**$\Delta_1/\ \Delta_f$**	**$\Delta_2/\ \Delta_f$**
Doherty et al. (2002)	13%	40%
Derakhshan, Ingham, and Griffith (2009)	1%	25%
Derakhshan and Ingham (2008)	2%	60%
Tested URM wall (Test #1)	**2%**	**52%**

Note that Doherty et al. (2002) defined in his model three degradation stages which were the criteria for determining the ratio of Δ_1/Δ_f and Δ_2/Δ_f. Considering this criteria, all the values presented in Table 1 were obtained assuming a moderate state of degradation.

As for the case of the first application, on this second application a specific weight value of 19 kN/m^3 was used. For test carried out in Test #1, the geometry used was that presented in Fig. 7(b). Applying Equation (1) for a force resultant at 1.305 m, a force of incipient rocking (F_0) of 19.09 kN is obtained. As exposed in section 2.2, in order to taking into account the low slenderness ratio of the wall, this value of force of incipient rocking obtained should be corrected by the sum of a compression force given by Equation (2). As exposed before, considering an angle of the internal friction of 38^o (according to Betti and Vignoli (2008)) and an horizontal cross section, A_v, of 1.05 m^2, for a maximum experimental force, F_{max}, of 19.24 kN, this compression force, R, is equal to 15.73 kN and consequently, the new force of incipient rocking, F_0, of 34.82 kN is obtained. Fig. 14 presents the confrontation between the experimental results obtained from Test #1 and the tri-linear model developed, considering the three energy based criteria presented in section 2.3.

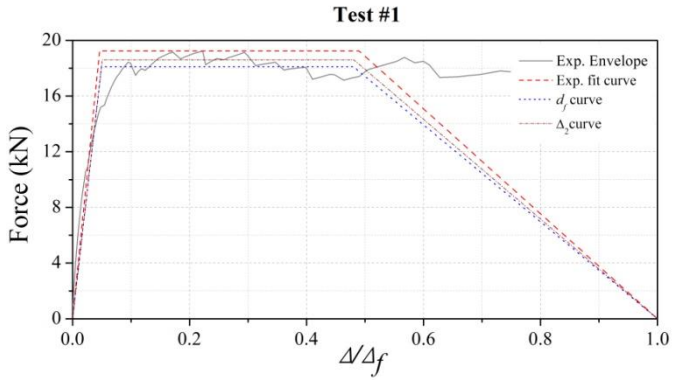

Fig. 14: Test #1: Experimental envelope vs. tri-linear model considering the energy based criteria proposed

For Test #2, and considering the geometrical configuration presented in A. A. Costa et al., (2011) – with a resultant applied at the high of 2.22 m –, a value of force of incipient rocking, F_0, of 13.61 kN is obtained. Finally for Test #3, considering a resultant at the high of 2.20 m, a value of force of incipient rocking F_0 of 18.41 kN is obtained. Note that these two values were obtained taking into account the partial participation of the lintels on the out-of-plane response of the pier by the development of shear forces on the lintels, V:

$$V = \tau_0 \times A_v \tag{3}$$

According to the Italian code (NTC2008, 2008) the value of the initial shear strength, τ_0, ranges between 20 and 30 kPa for the case of "*sacco*" stone masonry. According to the exposed, for the case Test #2 and Test #3, the force of incipient rocking was obtained by the sum of the value calculated through Eqn. (3) with the base shear force, V, affected with a correction factor, η, of 0.25 which regulates the participation of the lintels on the global response of the pier. Fig. 14 presents the confrontation between the experimental results obtained from the tests Test #2 and Test #3 and the tri-linear model developed.

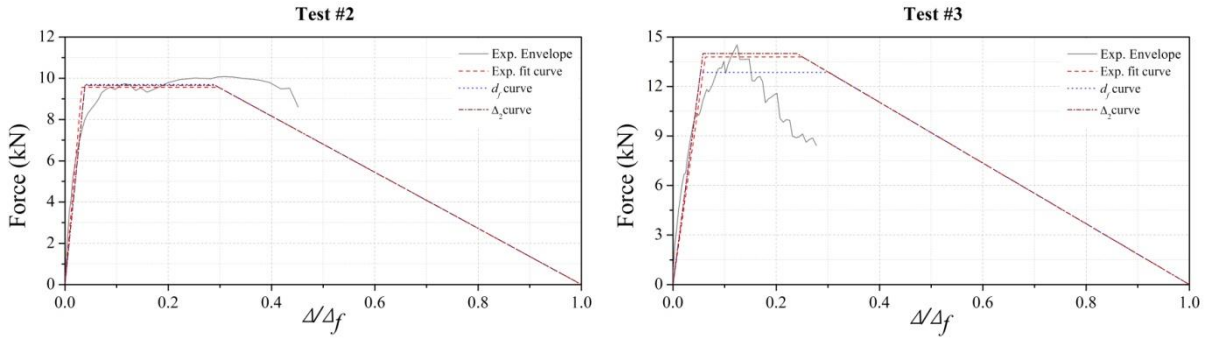

Fig. 15: Test #2 and Test #3: Experimental envelopes vs. tri-linear models

Table 2 presents the values of force and displacement obtained from the second application (presented above).

Table 2: Tri-linear model force and displacement parameters obtained for different energy based criteria

Energy based criterion "Experimental Fit Curve"

Test #	F_p (kN)	F_p/F_0	Δ_1 (mm)	Δ_2 (mm)	Δ_f (mm)	Δ_1/Δ_f (%)	Δ_2/Δ_f (%)
Test #1	18.28	0.51	11.10	117.58	0.24	4.63	48.99
Test #2	9.57	0.70	7.84	71.23	0.24	3.27	29.68
Test #3	13.79	0.75	15.03	60.20	0.24	6.26	25.08

Energy based criterion "d_f curve"

Test #	F_p (kN)	F_p/F_0	Δ_1 (mm)	Δ_2 (mm)	Δ_f (mm)	Δ_1/Δ_f (%)	Δ_2/Δ_f (%)
Test #1	18.11	0.52	11.88	115.18	0.24	4.95	47.99
Test #2	9.70	0.71	9.32	68.96	0.24	3.88	28.73
Test #3	12.85	0.70	12.79	72.49	0.24	5.33	30.20

Energy based criterion "Δ_2 curve"

Test #	F_p (kN)	F_p/F_0	Δ_1 (mm)	Δ_2 (mm)	Δ_f (mm)	Δ_1/Δ_f (%)	Δ_2/Δ_f (%)
Test #1	18.60	0.52	12.20	115.41	0.24	5.08	48.09
Test #2	9.65	0.71	9.27	69.84	0.24	3.86	29.10
Test #3	14.00	0.76	13.93	57.50	0.24	5.80	23.96

From the analysis of Table 1, it is possible to indicate new displacement values Δ_1 and Δ_2, calibrated for "*sacco"* stone masonry. As expected, for test 1 the ratio of $\Delta_2/\ \Delta_f$ cannot be directly compared with the same ratio obtained from Test #2 and Test #3. However, and comparing individually each one of these ratios, it is possible to state that these values vary significantly from the values suggested by other authors - (Doherty *et al.*, 2002); (Derakhshan *et al.*, 2009) and (Derakhshan & Ingham, 2008) – (see Table 2). Values ranging between 4% and 6% seem reasonable for ratio $\Delta_1/\ \Delta_f$. Taking into account only the test carried out in Test #1, values of $\Delta_2/\ \Delta_f$ about 50% seem appropriate. On the other hand, considering Test #2 and Test #3, this ratio decreases for values ranging between 30% and 40%.

Table 3 resumes the confrontation between the values obtained in this work and the values proposed in the literature.

Table 3: Different proposed $\Delta_i/\ \Delta_f$ ratios for the tri-linear model parameters

	Parameter	
Reference	$\boldsymbol{\Delta_1/\ \Delta_f}$	$\boldsymbol{\Delta_2/\ \Delta_f}$
Doherty et al. (2002)	13%	40%
Derakhshan, Ingham, and Griffith (2009)	1%	25%
Derakhshan and Ingham (2008)	2%	60%
URM wall (for distributed loads)	**4%-6%**	**50%**
URM wall (for point loads at the top)	**4%-6%**	**30%-40%**

In order to calibrate these and other tri-linear parameters, a new experimental laboratory test campaign is being prepared (see Fig. 16). Additionally, this new test campaign will allow investigate the influence of the test setup and the number of displacement cycles per test over the tri-linear model. This campaign involves the test of six similar stone masonry walls, three of them tested with an airbag test setup – distributed load – and the remaining three with a point load at the top.

Fig. 16: Construction images of the specimens

4 FINAL REMARKS

The importance of out-of-plane seismic response of URM walls was emphasized with a particular reference to the characteristics of URM buildings in Azores, Portugal. The application of a simplified displacement-based procedure has been presented. According to this procedure, tri-linear models based on three different energy base criteria were constructed in order to match the results experimentally obtained in three experimental tests. Moreover, the presentation of a recent *in situ* experimental campaign carried out has been reported, where the application of cyclic loads resorting to an airbag system.

The parameters obtained to construct the tri-linear model were then confronted with values proposed in the literature. Due to their high dispersion, the results obtained need extra validation resourcing to laboratory testing, which will be the next step to be taken.

5 FORTHCOMING DEVELOPMENTS

In order to calibrate the ultimate displacement, Δ_f, a new experimental campaign test is being prepared. This campaign will take place next September, in LESE laboratory. Six full-scale stone masonry piers will be tested, allowing study both the influence of the test setup and the number of the experimental cycles in the tri-linear results. Additionally, a new fatigue model is intended to be developed in order to uniform the application and the prediction of the experimental results.

ACKNOWLEDGEMENT

This work refers to research made with a financial contribution of the Portuguese Foundation for Science and Technology (FCT) under the project PTDC/ECM/104520/2008. The authors also thank the support of the Regional Government of Azores and the work of the technicians of the Laboratory of Earthquake and Structural Engineering in the experimental activity reported.

REFERENCES

Betti, M., & Vignoli, A. (2008). Modelling and analysis of a Romanesque church under earthquake loading: Assessment of seismic resistance. *Engineering Structures*, *30*(2), 352-367. doi:10.1016/j.engstruct.2007.03.027

Blaikie, E. L., & Davey, R. A. (2002). *Methodology for Assessing the seismic Performance of Unreinforced Masonry Single Storey Walls, Parapets and Free Standing Walls*. Report prepared

by OPUS International Consultants for the EQC Research Foundation: OPUS International Consultants.

Costa, A. (2002). Determination of mechanical properties of traditional masonry walls in dwellings of Faial Island, Azores. *Earthquake Engineering & Structural Dynamics*, *31*(7), 1361-1382. John Wiley & Sons, Ltd. doi:10.1002/eqe.167

Costa, A. A. (2012). *Seismic Assessment of the out-of-plane performance of traditional stone masonry walls*. PhD thesis. Faculdade de Engenharia da Universidade do Porto.

Costa, A. A., Arêde, A., Costa, A., & Oliveira, C. S. (2011). In situ cyclic tests on existing stone masonry walls and strengthening solutions. *Earthquake Engineering & Structural Dynamics*, *40*(4), 449-471. John Wiley & Sons, Ltd. doi:10.1002/eqe.1046

Derakhshan, H., & Ingham, J. M. (2008). Out-of-Plane testing of an unreinforced masonry wall subjected to one-way bending. *Australian Earthquake Engineering Conference, AEES 2008*. Retrieved from http://www.aees.org.au/Proceedings/2008_Papers/24_Derakhshan.pdf

Derakhshan, H., Ingham, J. M., & Griffith, M. C. (2009). Tri-linear force-displacement models representative of outof-plane unreinforced masonry wall behaviour. *11th Canadian Masonry Symposium, Toronto, Ontario, May 31-June 3*. Toronto, Ontario. Retrieved from http://www.retrofitsolutions.org.nz/pdfs/Canadian Masonry Symposium 2009- Hossein.pdf

Doherty, K., Griffith, M. C., Lam, N. T. K., & Wilson, J. L. (2002). Displacement-based analysis for out-of-plane bending of seismically loaded unreinforced masonry walls. *Earthquake Engineering and Structural Dynamics*, *31*(4), 833-50. Retrieved from http://en.scientificcommons.org/52922555

Griffith, M. C., Vaculik, J., Lam, N. T. K., Wilson, J., & Lumantarna, E. (2007). Cyclic testing of unreinforced masonry walls in two-way bending. *Earthquake Engineering & Structural Dynamics*, *36*(6), 801-821. John Wiley & Sons, Ltd. doi:10.1002/eqe.654

Kelly, T. (1995). Earthquake resistance of unreinforced masonry buildings. *Proc Annual Technical Conference of the NZ National Society for Earthquake Engineering* (pp. 28-35).

Lam, N. T. K., Griffith, M. C., Wilson, J. L., & Doherty, K. (2003). Time-history analysis of URM walls in out-of-plane flexure. *Engineering structures*, *25*(6), 743–754. Elsevier. Retrieved from http://www.sciencedirect.com/science/article/pii/S0141029602002183

Lam, N. T. K., Wilson, J. L., & Hutchinson, G. L. (1995). The seismic resistance of unreinforced masonry cantilever walls in low seismicity areas. *Bulletin of the New Zealand National Society for Earthquake Engineering*, *28*(3), 179-195. New Zealand National Society for Earthquake Engineering.

NTC2008. (2008). Norme tecniche per le costruzioni. D.M. 14 Gennaio 2008.

Tomaževič, M. (1999). *Earthquake-resistant design of masonry buildings. Series on Innovation in Structures and Construction - Vol. 1*. Imperial College Press, London.